

Characterization of large area photomultipliers and its application to dark matter search with noble liquid detectors

A. Bueno, J. Lozano, A.J. Melgarejo, F.J. Muñoz, J.L. Navarro, S. Navas* and A.G. Ruiz

*Dpto. de Física Teórica y del Cosmos & C.A.F.P.E., Universidad de Granada,
Campus Fuente Nueva, 18071 Granada, Spain
E-mail: navas@ugr.es*

ABSTRACT: There is growing interest in the use of noble liquid detectors to study particle properties and search for new phenomena. In particular, these detectors are extremely suitable for performing direct searches for dark matter. In this kind of experiment, the light produced after an interaction within the sensitive volume is usually read-out by photomultipliers. The need to go to masses in the tonne scale to explore deeper regions of the parameter space, calls for the use of large area photomultipliers. In this paper we address the need to perform laboratory calibration measurements of these large photomultipliers, in particular to characterize their behaviour at cryogenic temperatures where no reference data from the manufacturer is available. We present comparative tests of phototubes from two companies. The tests are performed in conditions similar to those of operation in a real experiment. Measurements of the most relevant phototube parameters (quantum efficiency, gain, linearity, etc.) both at room and liquid Argon temperatures are reported. The results show that the studied phototubes comply with the stringent requirements posed by current dark matter searches performed with noble-liquid detectors.

KEYWORDS: Photon detectors for UV, visible and IR photons (vacuum) (photomultipliers, HPDs, others); Cryogenic detectors; Detectors for UV, visible and IR photons.

*Corresponding author.

Contents

1. Introduction	1
2. PMT requirements	2
3. Measurements	4
3.1 Quantum Efficiency	4
3.1.1 Quantum Efficiency at room temperature	5
3.1.2 Quantum Efficiency at LAr temperature	6
3.2 Response to single photoelectrons (SER)	10
3.2.1 Experimental setup	10
3.2.2 Gain	10
3.2.3 Peak to Valley ratio and SER resolution	12
3.3 Dark counts	13
3.4 Linearity	14
4. Conclusions	15

1. Introduction

Particle interactions in liquefied noble gases produce charge by means of *ionization* of the atoms of the medium and *light*, by the de-excitation of the formed dimers [1]. This makes this class of detector a suitable tool to search for new physics. In particular, they represent a competitive technology in the quest for dark matter [2], since in this kind of experiment it is crucial to have several independent observables in order to suppress background events.

There are several ways to collect both charge and light [3] in noble liquid detectors. For light readout, the use of photomultiplier tubes (PMTs) is highly recommended as their time resolution allows to distinguish photons produced in a triplet state dimer (slow component) from those produced in a singlet state (fast component) [4]. This helps to improve background rejection capabilities.

Considering liquid Argon (LAr) as the sensitive medium, the intensity of the light produced is peaked at ~ 128 nm (see figure 1). This presents technical difficulties for PMTs, since conventional window glasses do not allow the passage of such a short wavelength. To avoid this inconvenient, usually either the inner detector surface or the PMT window is covered with a wavelength shifter, a substance able to absorb and re-emit the light on a longer wavelength. One of the most used wavelength shifters is the Tetraphenylbutadiene (TPB), which re-emits the light at wavelengths around 420 nm [5].

Therefore, PMTs are a crucial element of noble-liquid detectors. Even though the manufacturers provide data for each PMT model (gain, dark current, linearity, etc.), the values presented in the

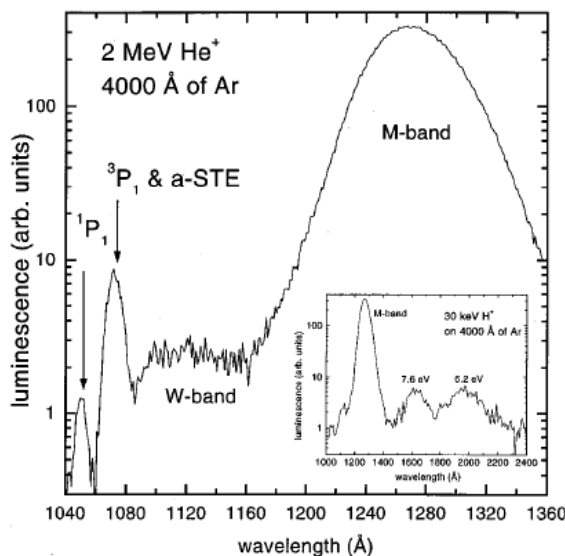


Figure 1. Argon emission spectrum reproduced from reference [6].

specification data sheet are usually too generic, based on averages over many PMTs, not specific to the purchased one. Non negligible deviations from the average behaviour can be expected for a particular PMT. Moreover, companies do not usually provide calibration data at cryogenic temperatures (~ 87 K for liquid Argon). For these reasons PMTs must be characterized individually as precisely as possible in the laboratory.

Currently running noble liquid dark matter detectors like WARP [7] and XENON [8], employ small size phototubes ($\sim 2''$ window) because of their relative small active volume (few liters). As a result of the scaling up of future detectors to improve dark matter detection capabilities, the size of the installed photomultipliers will probably be increased: the use of larger photocathode PMTs will allow coverage of bigger surfaces at lower cost. Indeed, the design of new prototypes like ArDM [9] (one tonne of LAr) already incorporates the use of large area photocathode tubes ($8''$ window). The work presented in this paper is focused on the study of those *large area* photomultipliers and how they behave when operated at cryogenic temperatures.

In this paper, we first discuss the general features required for a PMT as light sensor in a noble liquid dark matter detector and present the nominal characteristics of the tested tubes (section 2). The results of the main measurements performed on them are described in section 3: quantum efficiency (3.1), single photoelectron spectrum (3.2), dark counts (3.3) and linearity (3.4). Conclusions are reported in section 4.

2. PMT requirements

In the framework of noble liquid dark matter experiments, the first property required for a PMT is, obviously, to work properly at cryogenic temperatures $O(100$ K). This strong requirement is generally not satisfied by conventional PMTs. Photocathodes are usually semiconductors, thus when temperature is reduced to such low values, the cathode resistance can increase by several

orders of magnitude. This can cause a large voltage gradient in the photocathode, resulting in a poor collection efficiency at the first dynode [10, 11]. To avoid this undesirable effect the photocathode has to be deposited on a conducting substrate. Some companies are able to manufacture special coated PMTs for cryogenic applications.

Another important requirement is a good PMT response over a wide range of illumination levels. Signals ranging from the single photoelectron (pe) up to several hundreds of photoelectrons (if the particle interaction takes place close to the photocathode) can be expected in large detectors. An adequate PMT gain (G) should allow the detection of both types of events. The peak voltage of a signal can be estimated considering that the output charge of the anode will follow a Gaussian distribution in time, with RMS equal to the transit time spread of the electrons. If we assume a $50\ \Omega$ coupling between the anode and the electronics, then the integral of the output signal will be $50 \cdot G \cdot q$, with q the electron charge. The signal amplitude can be approximated by $A \sim 50 \cdot G \cdot q/TTS$ which for a 10^7 gain and a typical transit time spread (TTS) of 5 ns (for the considered ETL and Hamamatsu PMTs the values are 4 ns and 2.4 ns respectively [12, 13]) gives 16 mV output peak voltage. Hence, a nominal gain close to this value would fulfill the requirements in the 1–100 photoelectrons range. As explained later in the text, the gain is extracted from the single photoelectron charge spectrum, the so called Single Electron Response (SER), obtained with very low illumination levels. Besides the gain, the single photoelectron charge spectrum allows the study and characterization of other important PMT parameters (peak to valley, peak spread, etc.) which determine, for instance, the PMT energy resolution [14].

In order to estimate the number of photoelectrons produced in a single event, the response of the PMT should also be proportional to the incident light intensity. Deviations from the ideal behavior are primarily caused by anode linearity characteristics which, for pulsed sources it is mainly limited by space charge effects due to the magnitude of the signal current. An intense light pulse increases the space charge density and causes current saturation. Linearity should be at least granted up to levels of 100 pe.

Dark counts are signals that appear in the absence of light and that are caused by thermoionic emission [15], leakage currents, glass envelope scintillation, field emission current, residual gases, and radioactivity from the glass or the environment. PMTs may be used as well for triggering and although most of the dark counts will be suppressed by time coincidence between several PMTs, a low rate is desirable.

Concerning the spectral response of the PMT, as mentioned previously, the scintillation light emitted by excited Argon dimers has a wavelength peak at ~ 128 nm, where standard PMTs are blind. Only tubes made of MgF_2 windows extend the range of visibility down to 110 nm. Unfortunately, at the moment no large photocathode PMTs (8") are manufactured with this special type of window, so typical experiments make use of coating materials like TPB to shift the light to the 400–450 nm region where the PMT shows its best performance in terms of quantum efficiency (QE). This is a crucial parameter for dark matter experiments where very dim signals are recorded.

The timing resolution is another property which characterizes the PMT performances but this parameter does not seem to be an issue. Large photocathode PMTs actually present in the market show TTS values in the order of few ns, fast enough for the requirements of a dark matter detector.

Finally, the phototubes must be placed inside the detector sensitive volume so they should be manufactured using special low background materials. Natural radioactivity from material com-

Table 1. PMT models tested in this work (values from manufacturer generic data sheet).

Manufacturer	Model	Size	Gain	TTS	Dark Currents	QE (@ 420nm)
ETL	9357 KFLB	8"	1.1×10^7	4 ns	10 nA	18%
Hamamatsu	R-5912-MOD	8"	10^7	2.4 ns	50 nA	22%

pounds is a continuous source, among others, of low energy neutron and alpha particles which are the most pernicious source of background. Companies are able to manufacture a low background version of many PMT models under request.

Among the companies surveyed, only Electron Tubes Limited [12] and Hamamatsu [13] can offer large photocathode PMTs suitable to work under cryogenic conditions. Out of the available models, we have chosen those closest to the required specifications: the 9357-KFLB from Electron Tubes Limited (ETL) and the R-5912-MOD from Hamamatsu.

Two units of each model have been tested. Their main properties are summarized in table 1. In particular, they have nominal gains around 10^7 and peak quantum efficiencies close to 20%. Both models can be manufactured in low background glass.

Hereafter, the tested ETL and Hamamatsu phototubes will be referred to as ETL1, ETL2 and HAM1, HAM2 respectively.

The voltage dividers have been made using a custom PCB double-sided printed circuit board following the design provided by each manufacturer. In order to avoid changes in the values of the different components of the voltage divider at cryogenic temperatures, specially manufactured electronic resistors and capacitors with guaranteed stability up to LAr temperatures have been used [16].

3. Measurements

3.1 Quantum Efficiency

A precise knowledge of the PMT quantum efficiency as function of the incident photon wavelength will be of major importance for a dark matter detector which aims to exploit the full capabilities of a PMT, not only the trigger potential as a fast light detector but also the calorimetric ones. Among other variables, the parameterisation of QE as a function of λ is needed to infer the total amount of scintillation light released inside the active detector volume, following a particle interaction.

The method used for measuring the spectral response of the PMT is based on the comparison of its output signal with the response of a calibrated detector, in our case a photodiode. This measurement can be done by interchanging the calibrated and the unknown photosensor after each measurement at a fixed value of λ , or by splitting the light beam in two and taking both measurements simultaneously. In order to minimize the errors induced by the light source instabilities and misalignments of the devices, the second method was followed.

As explained in section 3.1.2, the measurement is done, first, at room temperature (*hot* spectral response) and then combined with the data obtained in liquid Argon to compute the final value *in cold*. As expected, it is found that the quantum efficiency properties of the tested PMTs change sub-

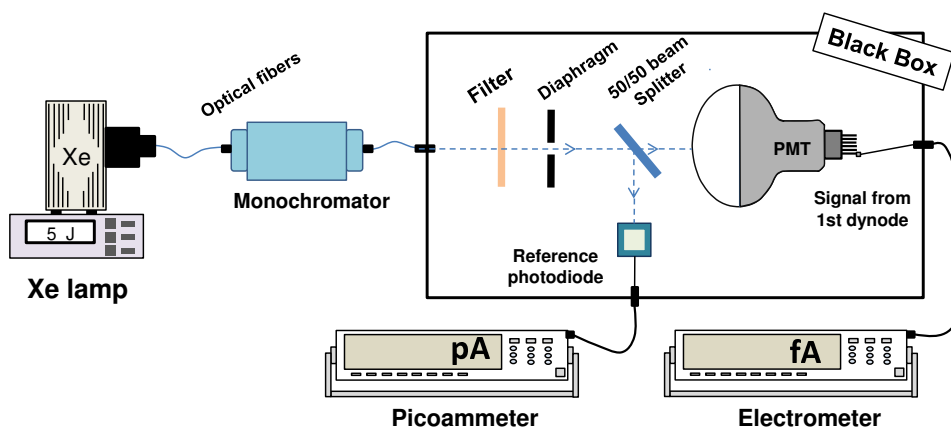


Figure 2. Schematic drawing of the setup used for quantum efficiency measurements at room temperature.

stantially with temperature, so a careful measurement of $QE(\lambda)$ in cryogenic conditions is mandatory.

Sections 3.1.1 and 3.1.2 describe the measurements done at the cryogenic laboratory of the University of Granada and the obtained results on the quantum efficiency measurements at room and LAr temperatures, respectively.

3.1.1 Quantum Efficiency at room temperature

Figure 2 shows the experimental setup used to measure the quantum efficiency at room temperature. It is mainly composed of a light source, a monochromator and a light-tight box where the photosensors are placed.

The light source should provide an spectral distribution covering the range of interest (300 nm–600 nm) with a high light intensity. The ORIEL Newport 6427 Xenon lamp [17] matches those requirements. It can be used in pulsed mode (max. energy of 5 J) and the output can be easily coupled to the monochromator by means of an optical fiber. The stability of the lamp has been tested by measuring its output flux during several hours and it has shown deviations below 1 % in time slots of 5 minutes (duration of a single QE measurement). The lamp is also equipped with a shutter.

The monochromator (Spectral Products Digikrom CM110 CVI [18]), controlled with a computer via the RS-232 port, is equipped with a 2400 g/mm grating which allows the selection of a particular wavelength between 180 and 680 nm (peak at 240 nm) with an accuracy of ± 0.6 nm.

A second optical fiber is used to send the monochromatic light into the aluminum box which provides a completely dark environment and acts as a Faraday cage. The box houses a filter (to block any shorter *harmonic* wavelength from the monochromator), a diaphragm (to reduce the size of the light spot, such that it completely fits inside the photodiode sensitive area), a 50/50 Polka-dot beam splitter (by Edmund Optics [19]) and the two photosensors. The reference detector is a Hamamatsu S1337-1010BQ photodiode, with 10×10 mm² active area. It has been calibrated by the manufacturer. The setup is completed with two devices to measure independently the current

produced by the reference photodiode and the photocathode of the tested PMTs: a Picoammeter (mod. 6485) and a Electrometer (mod. 6514) both from Keithley [20].

The quantum efficiency measurement comes from the comparison of the currents produced in the photodiode and in the first dynode of the unknown PMT. In order to ensure an optimal collection efficiency between the photocathode (K) and the first dynode (D_1), a gradient of $\Delta V_{K-D_1} = 300$ V is kept between these two points. Even in absence of light, this gradient generates a small leakage current (~ 10 pA) which must be subtracted from the measurements in presence of light (shutter lamp open).

In order to get rid of systematic effects coming from the beam splitter inaccuracy (5% according to the manufacturer) two measurements were carried out exchanging the positions of PMT and photodiode. The geometric average of both measurements is taken as the final value. Indeed, in the configuration shown in figure 2, the photodiode receives a fraction α of the incident light measuring an intensity I^r (reflected in the splitter) whereas the PMT receives the transmitted one ($1-\alpha$) and measures I^t . We can write:

$$\frac{I_{\text{PMT}}^t}{QE_{\text{PMT}} \cdot (1 - \alpha)} = \frac{I_{\text{PD}}^r}{QE_{\text{PD}} \cdot \alpha} \quad (3.1)$$

When the two photodetectors are exchanged:

$$\frac{I_{\text{PMT}}^r}{QE_{\text{PMT}} \cdot \alpha} = \frac{I_{\text{PD}}^t}{QE_{\text{PD}} \cdot (1 - \alpha)} \quad (3.2)$$

Combining equations (3.2) and (3.1) it follows:

$$QE_{\text{PMT}} = QE_{\text{PD}} \cdot \sqrt{\frac{I_{\text{PMT}}^r}{I_{\text{PD}}^r} \frac{I_{\text{PMT}}^t}{I_{\text{PD}}^t}} \quad (3.3)$$

which is independent of the beam splitter accuracy.

Figure 3 shows the results obtained for the measurements of quantum efficiency at room temperature.

The points, in steps of 10 nm, follow a smooth curve. The quantum efficiency shows maximum values in the range 15–20% for a wavelength of about 400 nm. In the vicinity of the peak, the Hamamatsu models show an almost flat region between 350–450 nm, whereas the ETL PMTs present a steeper behaviour.

3.1.2 Quantum Efficiency at LAr temperature

To perform the measurements *in cold*, the previous experimental setup has to be slightly modified (see figure 4). This measurement requires the tested PMT to be fully immersed in liquid Argon for long periods of time (several hours). A special light-tight cryostat is used for that purpose, ensuring stable temperature conditions. It is equipped with three feedthroughs: one for LAr filling, a second one to feed the 1st dynode and read-out the current with the Electrometer, and the third one to pass the optical fiber which illuminates the PMT. Inside the cryostat, the fiber is positioned very close to the PMT surface such that dispersion effects due to a change of the medium conditions are negligible. A specially designed supporting structure made of stainless steel and polyethylene disks houses the PMT and fixes the fiber inside the cryostat.

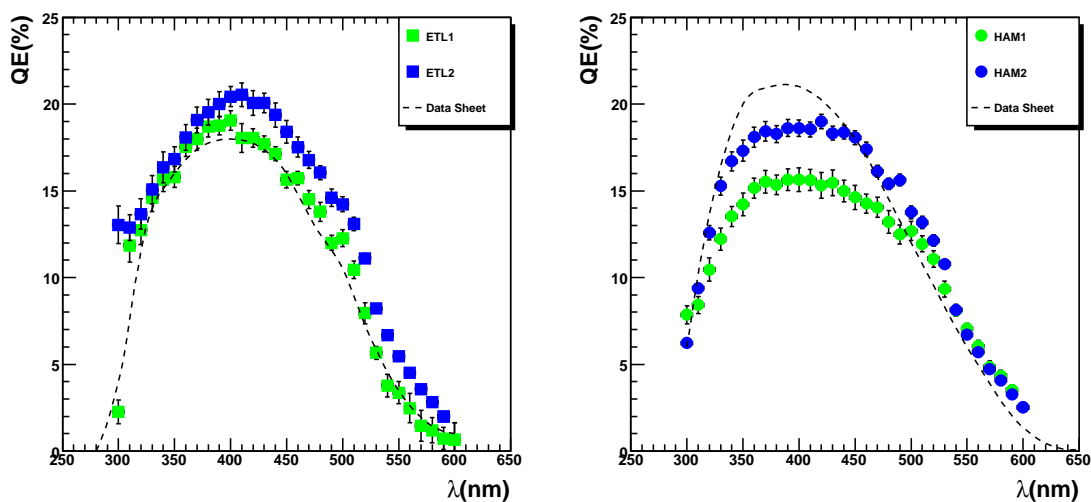


Figure 3. Quantum efficiency of the ETL (left) and Hamamatsu (right) PMTs as measured at room temperature. Curves from manufacturers are included. Hamamatsu data are for a PMT without Pt underlayer, which accounts for the observed differences.

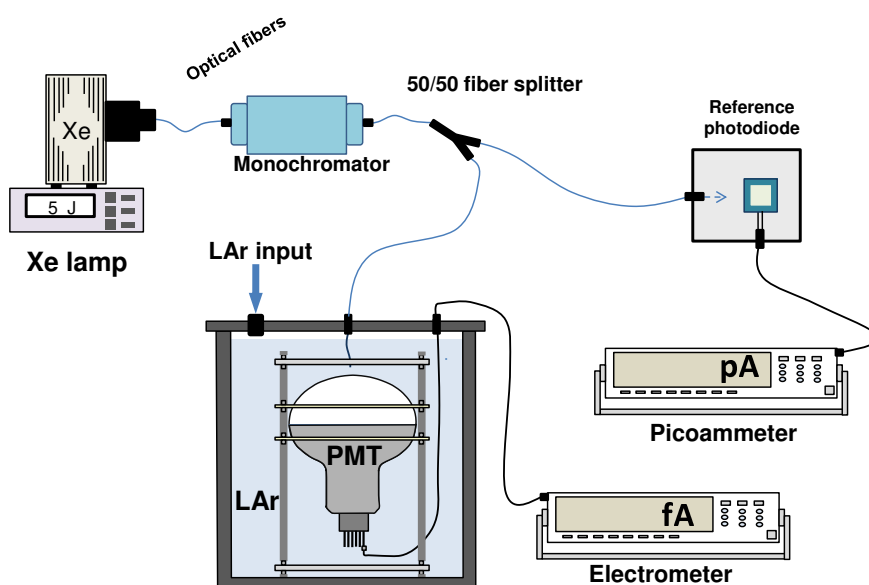


Figure 4. Schematic drawing of the setup used for quantum efficiency measurements at LAr temperature.

On the other hand, the Hamamatsu S1337-1010BQ reference photodiode remains at room temperature in order to keep valid the manufacturer calibration. It is placed inside an aluminum light-tight box.

The Xe lamp, the monochromator and the charge readout devices are the same as in 3.1.1. The Polka-dot beam splitter is replaced by a 50/50 optical fiber splitter (Ocean Optics) allowing a stable light flux between the monochromator and the two photosensors.

A first measurement is done with the PMT in air, at room temperature, where the intensity generated in the photodiode $I_{\text{PD}}^{\text{hot}}$ can be written as:

$$I_{\text{PD}}^{\text{hot}} = N_r \cdot \alpha \cdot QE_{\text{PD}} \quad (3.4)$$

N_r being the number of photons per unit of time before entering the fiber splitter, and α the fraction of photons split to the photodiode. This is kept at room temperature during the whole procedure, therefore the labels *hot* and *cold* are just used to distinguish the two measurements. An important difference respect to the previous measurement is that in this case only one measurement of the cold quantum efficiency is done, being the other one a reference measurement of the hot quantum efficiency. Hence, no mean will appear in the final expression for the QE.

The intensity in the PMT, I_{PMT} , will be given by:

$$I_{\text{PMT}}^{\text{hot}} = N_r \cdot (1 - \alpha) \cdot QE_{\text{PMT}}^{\text{hot}} \quad (3.5)$$

Combining both equations:

$$\frac{I_{\text{PMT}}^{\text{hot}}}{(1 - \alpha) \cdot QE_{\text{PMT}}^{\text{hot}}} = \frac{I_{\text{PD}}^{\text{hot}}}{\alpha \cdot QE_{\text{PD}}} \quad (3.6)$$

Once the spectral response is measured at room temperature, the cryostat is filled with LAr. The time needed for the PMT and the sustaining structure to cool down and stop boiling is about 1 hour. After that, the set of measurements is repeated and an analogous expression can be written:

$$\frac{I_{\text{PMT}}^{\text{cold}}}{(1 - \alpha) \cdot QE_{\text{PMT}}^{\text{cold}}} = \frac{I_{\text{PD}}^{\text{cold}}}{\alpha \cdot QE_{\text{PD}}} \quad (3.7)$$

Assuming the fraction α and the photodiode quantum efficiency constant during the whole procedure, the combination of equations (3.6) and (3.7) provides the following expression for the QE at LAr temperature:

$$QE_{\text{PMT}}^{\text{cold}} = QE_{\text{PMT}}^{\text{hot}} \cdot \frac{I_{\text{PD}}^{\text{hot}} \cdot I_{\text{PMT}}^{\text{cold}}}{I_{\text{PD}}^{\text{cold}} \cdot I_{\text{PMT}}^{\text{hot}}} \quad (3.8)$$

Since measurements of QE^{cold} are correlated to those at room temperature, errors have to be properly propagated. Figure 5 shows the QE results obtained for the tested PMTs. For what concerns dark matter interactions, quantum efficiencies around 20% guarantee, for geometries like the one foreseen for the ArDM experiment, yields of about 1 photoelectron per keV of deposited energy. This is enough to identify signals down to true recoil energies of 20 to 30 keV.

As compared to room temperature, a shift of the peak towards shorter wavelengths and an increase of the absolute QE at the maximum is observed in all cases. This effect is more clearly visible in figure 6, where the relative change from room to cryogenic temperature $\left[100 \cdot \left(1 - \frac{QE_{\text{cold}}}{QE_{\text{hot}}}\right)\right]$ is shown.

This behaviour [11, 21, 22] is related to the photoemission process [10] that takes place whenever a photon hits the photocathode of a PMT, usually a semiconductor (*bialkali* in the two tested models). When this happens, an electron is excited to the conduction band. The emission process is not a surface effect, but a bulk one. Hence, the electron must go through the semiconductor crystal until it reaches the vacuum, losing energy in each collision. If the electron reaches the

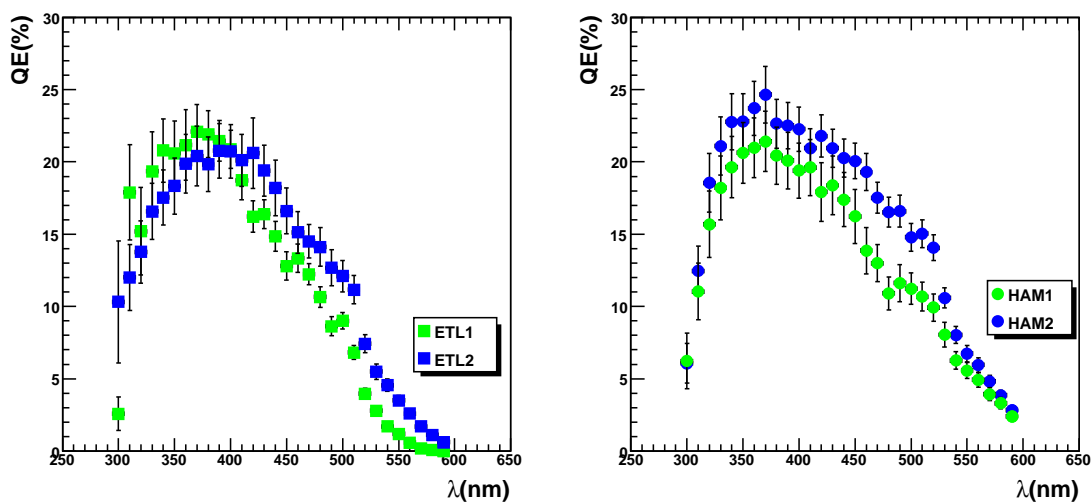


Figure 5. Quantum efficiency of the ETL (left) and Hamamatsu (right) PMTs as measured at cryogenic temperature.

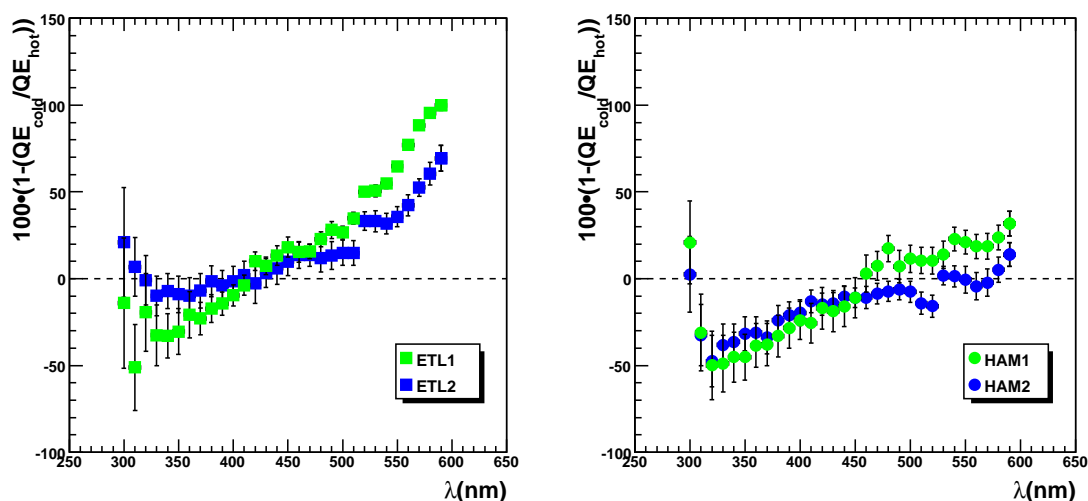


Figure 6. Change in quantum efficiency between room and cryogenic temperature for ETL (left) and Hamamatsu (right) models.

crystal surface with sufficient energy to escape over the potential barrier, it will be emitted from the photocathode. When temperature decreases, the yield from the photocathode increases in the region far from the cutoff wavelength, due to a decrease of the energy loss of the electron in the lattice. In the region close to the cutoff wavelength, above which the photoelectric process is not anymore feasible, the yield decreases because of a decrease in occupied defect levels above the valence band, an increase in band gap, and probably an unfavorable change in band bending.

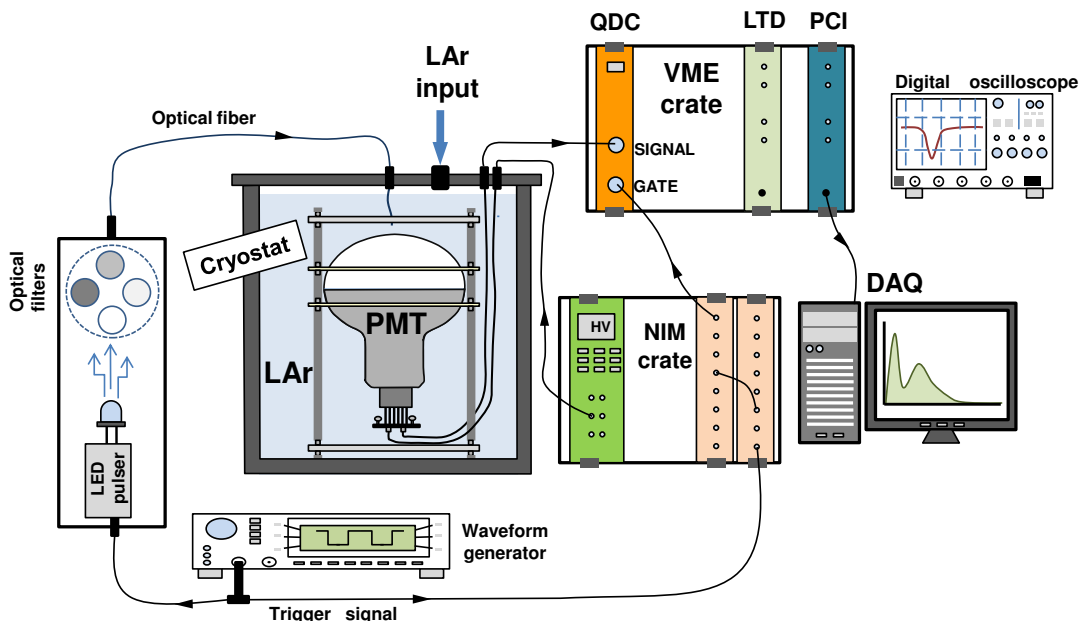


Figure 7. Setup for gain, dark counts and linearity measurements.

3.2 Response to single photoelectrons (SER)

3.2.1 Experimental setup

The setup used for single electron response, dark counts and linearity measurements is shown in figure 7. The PMT is housed inside a light-tight cryostat which can be filled with liquid Argon. The measurements were sequentially done first at room temperature and then in a LAr bath. The plots shown in this section only refer to results at cryogenic temperature, although some comments on comparisons with room temperature measurements are also included.

We use a standard LED with peak emission at 420 nm as light source and connect it to a pulser which provides 1 kHz frequency, few nanoseconds width light shots. If required, the light intensity can be attenuated by a set of neutral density filters. The light is sent to the PMT photocathode inside the cryostat thanks to an optical fiber. The PMT is biased with a NIM power supply (CAEN N470 [23]) and the signal transmitted through a standard LEMO cable. Depending on the measurement to be done, the signal is analyzed with a Charge-to-Digital Converter (QDC CAEN V965A), an oscilloscope (LeCroy Waverunner 6100) or a Low Threshold Discriminator (LTD CAEN V814B) plus a Scaler (CAEN V560AE).

3.2.2 Gain

To measure the PMT gain, the amount of light reaching the photocathode is reduced to the level of few photons. The number of generated photoelectrons follows a Poisson distribution and the probability of having r photoelectrons is expressed as:

$$P(r) = \mu^r \cdot \frac{e^{-\mu}}{r!} \quad (3.9)$$

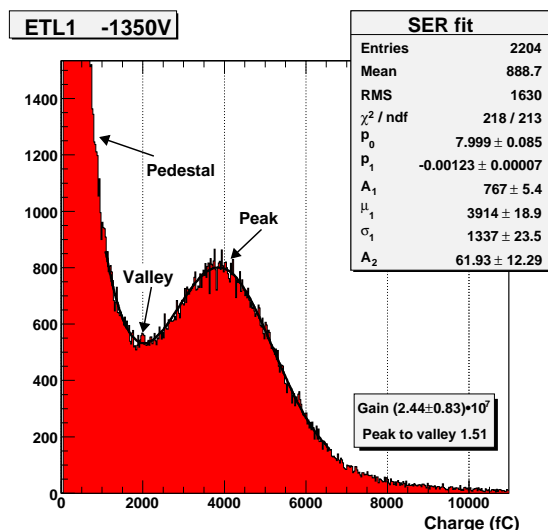


Figure 8. Example of a SER spectrum as obtained for the ETL1 at 1350 V.

The single photoelectron illumination level can be achieved by imposing that most of the signals come from single electron events i.e., by requiring the number of signals with two photoelectrons being below, for instance, 10% of that of single photoelectron. Using equation (3.9), the previous condition translates into $\mu = 0.2$ and $P(0) = 81.9\%$. Hence, if the light intensity is adjusted such that the number of empty triggers is 81.9% then the number of 2 photoelectrons signals will be one-tenth of that for 1 photoelectron. Under this condition, for any other number of photoelectrons the probability will be negligible.

Figure 8 shows an example of the collected charge spectrum under these conditions (SER) as obtained for ETL1 at 1350 V. The SER distribution has been fitted to a function which contains the following terms [11, 24]:

- An exponential distribution that fits the *pedestal steep fall* and which is caused by several factors: the continuous component of the dark current, the intrinsic shift of the QDC, the electronic noise affecting the measurement, etc. This exponential is parameterized as $e^{p_0+p_1 \cdot x}$.
- A Gaussian distribution which takes into account the response of the PMT to a single photoelectron (parameters A_1 , μ_1 and σ_1).
- An extra Gaussian with parameters A_2 , $\mu_2 = 2 \cdot \mu_1$ and $\sigma_2 = \sqrt{2} \cdot \sigma_1$ to account for events with 2 photoelectrons. In general, a sum of n Gaussians can be included to reproduce n -photoelectron contributions.

The gain is obtained from the position of the single photoelectron peak in the charge spectrum. Figure 9 shows the gain dependence on High Voltage (HV) for the four tested PMTs in cold. A clean linear behaviour is observed in all cases. The Hamamatsu tubes achieve the nominal 10^7 gain at about 1100 V whereas the ETL tubes need higher voltages. On the other hand, the slope for ETL PMTs is steeper. It is interesting to notice that similar values and slopes were measured at

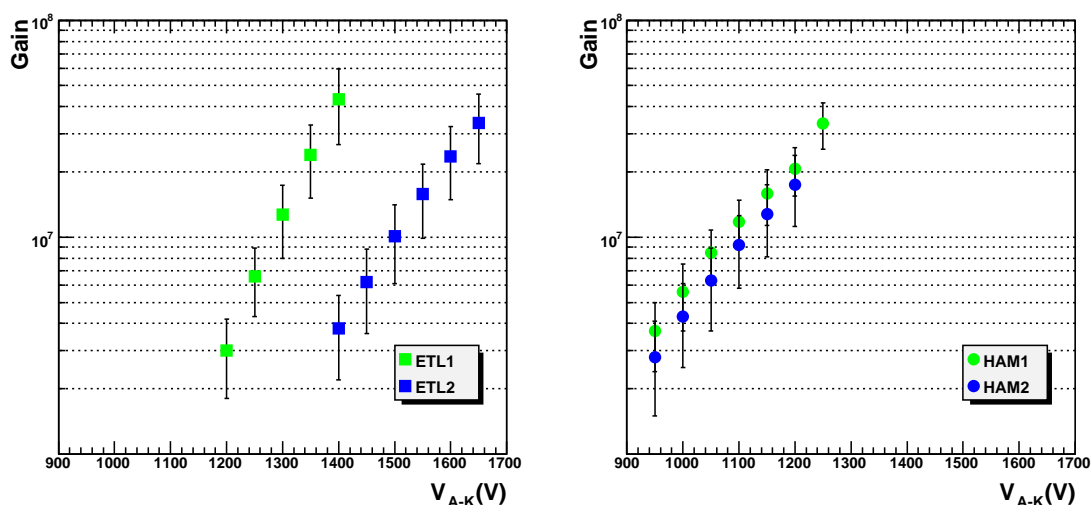


Figure 9. Gain dependence on HV for the four photomultipliers as measured in LAr.

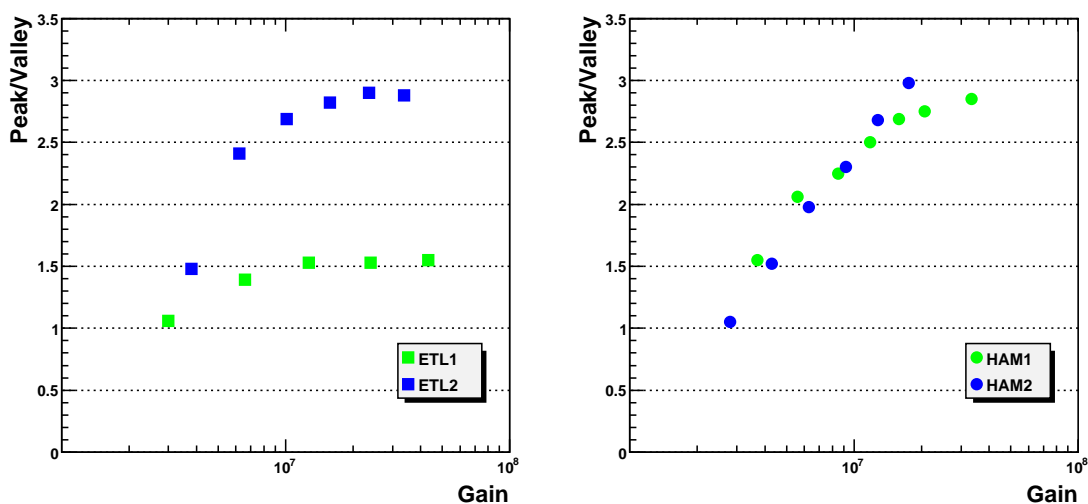


Figure 10. Peak to valley dependence on gain at LAr temperature.

room temperature. This uniformity on the results can be attributed to the stability of the cryogenic electronic components mounted on the PMT base.

3.2.3 Peak to Valley ratio and SER resolution

The ratio between the height of the single photoelectron peak and the valley (P/V), obtained from the charge spectrum (see figure 8) is another important characteristic to be measured. Figure 10 shows the results obtained on this quantity as a function of the gain.

The peak to valley ratio increases with gain in all cases. For a gain of 10^7 the measured value is around 2.5 for all PMTs but the ETL1, which shows a lower value. Beyond this point, the ETL tubes show an almost flat P/V while the Hamamatsu ones increase with voltage.

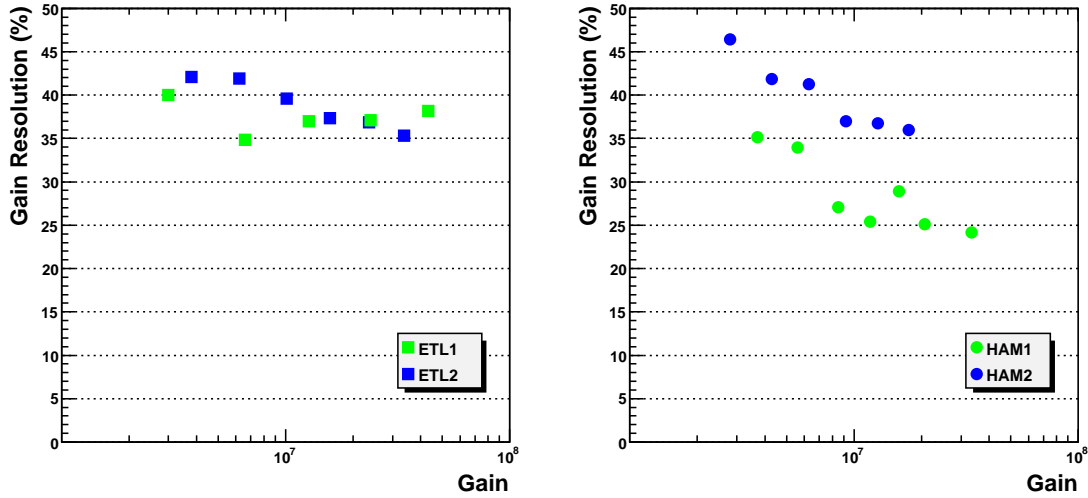


Figure 11. Gain resolution from SER spectrum for the tested PMTs at LAr temperature.

Figure 11 shows the resolution in the SER peak, defined as the ratio $\frac{\sigma_1}{\mu_1}$ in percentage. While the ETL tubes exhibit an almost flat dependence on the considered range, the resolution decreases smoothly on the Hamamatsu PMTs as gain is increased. At the nominal value of 10^7 the four tubes show resolution values in the range 35–40%.

3.3 Dark counts

Before measuring the dark count frequency, the phototubes are placed in darkness, inside the container filled with LAr and connected to the HV for several hours. The PMT output is then connected to the discriminator and the output signal is feed to a scaler (CAEN V560AE), where the number of pulses above a given threshold is counted. As an example, figure 12 shows the result for HAM1 biased at 1050 V.

To compare different PMTs at different voltages, thresholds in the discriminator (mV) have to be expressed in terms of number of photoelectrons in amplitude. The SER peak voltage is obtained from recorded oscilloscope signals taken at very low intensity illumination conditions. Looking at figure 12, the abrupt fall (factor 100) at low thresholds, corresponding to the level of single photoelectron, is clear. Beyond this point, the decrease in rate when increasing the threshold is smooth.

Figure 13 shows the number of dark counts for different values of gain above 4 photoelectrons for every PMT. This threshold has been selected as it is far from the abrupt fall region but it is still low enough to be used as a trigger.

As expected, the dark count rates increase with gain (higher voltages). Frequencies in the range 50–100 Hz are obtained for gain values around 10^7 .

Compared with the results at room temperature a clear decrease in the rates is measured *in cold*: a factor close to 5 and 2 for the ETL and Hamamatsu tubes, respectively. This effect is explained by the decrease of the thermal energy of the electrons in the photocathode.

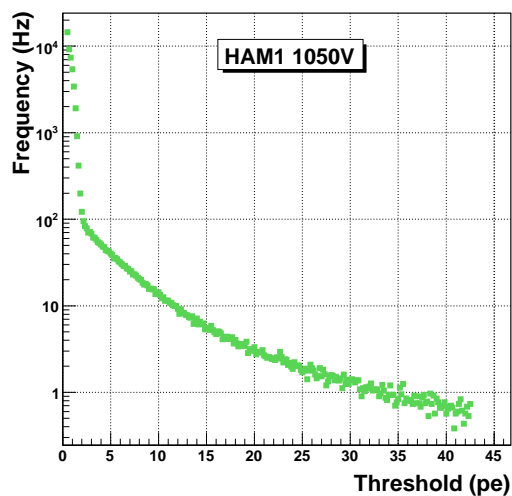


Figure 12. Dark counts rate dependence on discriminator threshold for HAM1 at 1050 V.

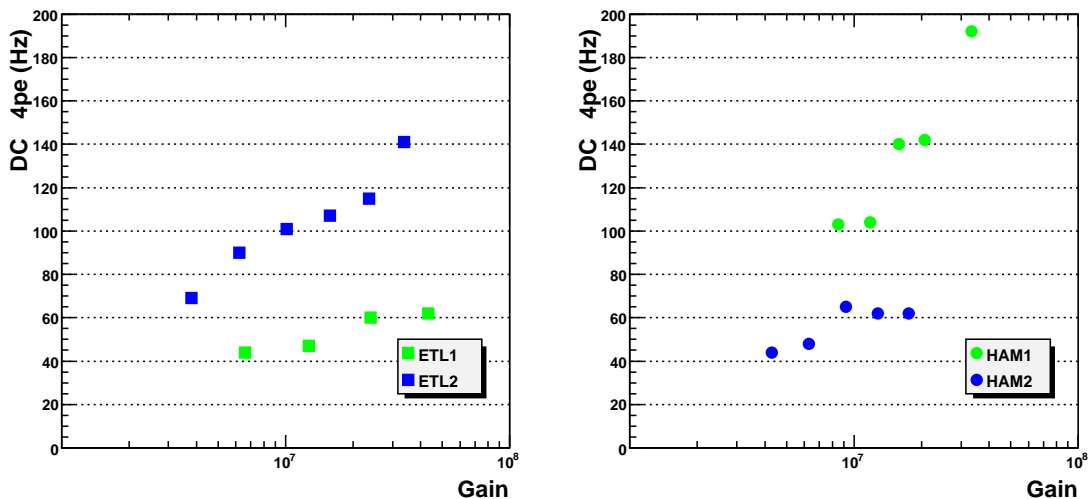


Figure 13. Dark counts rates as measured in LAr (4 pe threshold).

3.4 Linearity

The study of the PMT response to different illumination levels above the single photoelectron was carried out using neutral density filters [24]. They were placed in a rotating support, just between the light source (pulsed blue LED) and the optical fibre light guide (see figure 7). Five filters were used (optical density values $d = 3.0, 2.0, 1.5, 0.5$ and 0.3) which allowed variations of the light intensity brought to the photocathode by three orders of magnitude (attenuation factor = 10^d). The measurement proceeds as follows: the PMT voltage is adjusted to a gain of 10^7 and maintained unchanged, the higher optical density filter selected and the LED intensity tuned and fixed. In these conditions the average number of photoelectrons in the PMT is fixed between one and two. Then, a PMT charge spectrum is recorded with each filter and analyzed.

Figure 14 shows the kind of spectrum obtained by this method. If the parameters of the Gaus-

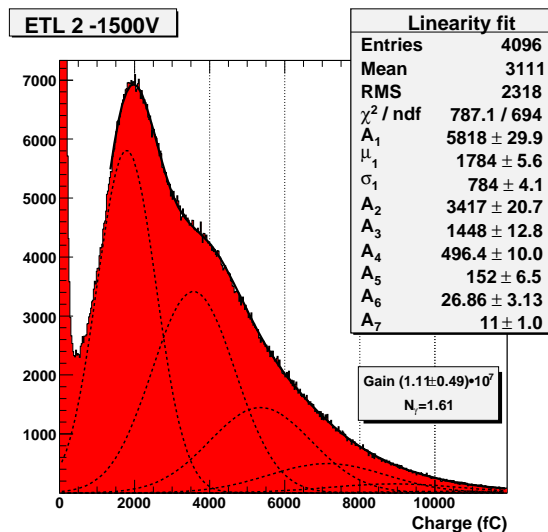


Figure 14. Example of charge spectrum (ETL2) obtained, during the linearity measurements, with the 3.0 optical density filter. Dotted lines (solid line) correspond to individual Gaussian fits (global fit).

sian for one photoelectron are μ_1 and σ_1 , the parameters of the distribution for the coincidence of n photoelectrons are given by the sum of the corresponding Gaussians, i.e. $\mu_n = n \cdot \mu_1$ and $\sigma_n = \sqrt{n} \cdot \sigma_1$. The average number of photons can be then computed as $\frac{\sum i \cdot N(i)}{\mu_1 \cdot \sum N(i)}$, where $N(i)$ is the content of the i -th bin of the charge distribution. For the measurement shown in figure 14, a value close to 1.6 is obtained. Dotted lines correspond to the first five Gaussians whereas the convolution (solid line) nicely follows the global data. The most left peak corresponds to the pedestal (empty trigger events).

In order to complete the linearity measurements, charge spectra with all neutral density filters are acquired. For very high photocathode illumination levels it is not possible anymore to resolve peaks for different number of photoelectrons and there are no empty trigger events, which requires a prior measurement of the pedestal. The ratio between the average charge in the distribution and the charge of a single photoelectron (from the $d = 3.0$ filter measurement) gives the mean number of photoelectrons.

A comparison between the ideal number of photoelectrons and the measured one can be obtained using the transmittance relationship between the filters. The result is shown in figure 15. The four PMTs show a nice linear behaviour up to 100 pe. Above this value a slight departure from linearity is clearly seen. However this is not a serious concern, since such large energy depositions are well above the energy window where we expect to see most of the signal due to interactions of dark matter components.

4. Conclusions

In this paper we have analyzed whether large-area phototubes are suitable for operation at cryogenic temperatures and fulfil the stringent physics requirements imposed by future dark matter experiments. Only two companies are able, nowadays, to provide PMTs capable of operating at

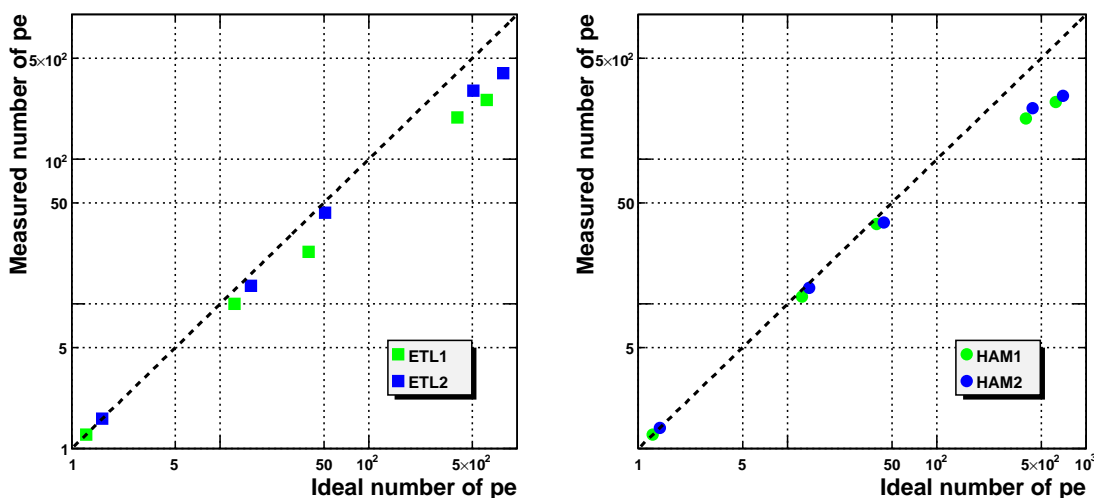


Figure 15. Linearity measurements: PMT signal in units of number of photoelectrons as function of the ideal one as measured in liquid argon. The dotted line shows the perfect linearity behaviour.

temperatures in the vicinity of hundred kelvins or lower. We have extensively tested 8” phototubes from ETL (9357 KFLB) and Hamamatsu (R-5912-MOD) both at room and liquid Argon temperatures. Our conclusion is that both models are adequate for installation in an experiment like ArDM, since they have QE above 20% for 400 nm, thus guaranteeing light yields of at least 1 pe/keV, enough to detect signals depositing around 20 to 30 keV. They show a linear behaviour throughout the energy window where we expect to have better chances to detect dark matter. In addition, their timing accuracy is such that they will allow to distinguish fast from slow scintillation light components, thus providing a powerful rejection tool against background.

Acknowledgments

This work has been supported by CICYT Grants FPA-2006-00684, FPA-2002-01835 and FPA-2005-07605-C02-01. We warmly thank our colleagues from the ArDM experiment for useful discussions and advise during the realization of these tests.

References

- [1] A. Hitachi et al., *Scintillation and ionization yield for α particles and fission fragments in liquid argon*, *Phys. Rev. A* **35** (1987) 3956.
- [2] R.J. Gaitskell, *Direct detection of dark matter*, *Ann. Rev. Nucl. Part. Sci.* **54** (2004) 315.
- [3] R. Bellazzini et al., *Imaging with the invisible light*, *Nucl. Instrum. Meth. A* **581** (2007) 246 [physics/0703176].
- [4] S. Kubota, M. Hishida and J. Raun, *Evidence for a triplet state of the self-trapped exciton states in liquid argon, krypton and xenon*, *J. Phys. C* **11** (1978) 2645.
- [5] W.M. Burton and B.A. Powell, *Fluorescence of tetraphenylbutadiene in the vacuum ultraviolet*, *Appl. Opt.* **12** (1973) 87.

- [6] D.E. Grosjean et al., *Absolute luminescence efficiency of ion-bombarded solid argon* *Phys. Rev. B* **56** (1997) 6975.
- [7] R. Brunetti et al., *WARP liquid argon detector for dark matter survey*, *New Astron. Rev.* **49** (2005) 265.
- [8] J. Angle et al., *First results from the XENON10 dark matter experiment at the Gran Sasso National Laboratory*, [astro-ph/0706.0039](http://arxiv.org/abs/astro-ph/0706.0039).
- [9] A. Rubbia, *ArDM: A ton-scale liquid argon experiment for direct detection of dark matter in the universe*, *J. Phys. Conf. Ser.* **39** (2006) 129 [[hep-ph/0510320](http://arxiv.org/abs/hep-ph/0510320)].
- [10] W.E. Spicer and F. Wooten, *Photoemission and photomultipliers*, *Proc. IEEE* **51** (1963) 1119.
- [11] A. Ankowski et al., *Characterization of ETL 93571a photomultiplier tubes for cryogenic temperature applications*, *Nucl. Instrum. Meth. A* **556** (2006) 146.
- [12] Electron Tubes Enterprises Limited, <http://www.electrontubes.com>.
- [13] Hamamatsu Photonics K.K., <http://www.hamamatsu.com>.
- [14] A. Ostankov et al., *A study of the new hemispherical 6-dynodes PMT from electron tubes*, *Nucl. Instrum. Meth. A* **442** (2000) 117.
- [15] Hamamatsu Photonics, *Photomultiplier tubes: basics and application*, 3rd ed. (2007).
- [16] Cryocircuits, <http://www.cryocircuits.com>.
- [17] Newport Oriel Instruments, <http://www.newport.com/oriel>.
- [18] Spectral Products, <http://www.spectralproducts.com>.
- [19] Edmund Optics, <http://www.edmundoptics.com>.
- [20] Keithley, <http://www.keithley.com>.
- [21] H.M. Araujo et al., *Study of bialkali photocathodes below room temperature in the UV/VUV region*, *IEEE Trans. Nucl. Sci.* **45** (1998) 542.
- [22] A.S. Singh and A.G. Wright, *The determination of photomultiplier temperature coefficients for gain and spectral sensitivity using the photon counting technique*, *IEEE Trans. Nucl. Sci.* **34** (1987) 434.
- [23] CAEN, <http://www.caen.it>.
- [24] R. Dossi et al., *Methods for precise photoelectron counting with photomultipliers*, *Nucl. Instrum. Meth. A* **451** (2000) 623.